RIF1 acts as a gatekeeper of B cell identity during late differentiation

Rahjouei A.[1#], Kabrani E.[1#], Berruezo-Llacuna M.[1,2], Altwasser R.[1,3], Delgado-Benito V.[1], Pavri R.[4], and Di Virgilio M.[1,5,*]

[1]Laboratory of Genome Diversification & Integrity, Max Delbrück Center for Molecular Medicine in the Helmholtz Association, Berlin 13125, Germany

[2]Humboldt-Universität zu Berlin, Berlin 10117, Germany

[3]Current address: Department of Hematology, Oncology, and Cancer Immunology, Charité-Universitätsmedizin Berlin, Berlin 10117, Germany

[4]Research Institute of Molecular Pathology (IMP), 1030 Vienna, Austria

[5]Charité-Universitätsmedizin Berlin, Berlin 10117, Germany

[#]These authors contributed equally

*Correspondence: michela.divirgilio@mdc-berlin.de

Abstract

RIF1 is a multifunctional protein that promotes immunoglobulin (Ig) isotype diversification. Whether RIF1 plays additional roles in adaptive immunity is unknown. In this study, we showed that *Rif1* expression is upregulated following mature B cell activation, while its deficiency skewed the transcriptional profile of activated B cells towards plasmablasts (PBs) and plasma cells (PCs). Additionally, RIF1 ablation resulted in increased PB formation *ex vivo* and enhanced terminal differentiation into PCs upon immunization. Therefore, RIF1 serves as a cell identity gatekeeper during late B cell differentiation, providing an additional layer of control in the establishment of humoral immunity.

Keywords: mature B cells, differentiation, plasma cells, RIF1, transcription, BLIMP1

Running Title: RIF1 restrains terminal B cell differentiation

Introduction

Mature B cells are the crucial cell type that delineates the two main B cell lineage development phases. During early B cell development in the bone marrow, common lymphoid progenitors develop into immature B cells *via* a step-wise process linked to the rearrangement of their antibody receptor/immunoglobulin (Ig) genes by V(D)J recombination (Lin et al. 2018; Nemazee 2017). Immature B cells expressing a functional and non-autoreactive B cell receptor (BCR) migrate to the periphery, where they complete their maturation into quiescent resting cells (Lin et al. 2018; Nemazee 2017). The encounter of these naïve mature B cells with their cognate antigen in secondary lymphoid organs triggers late B cell differentiation into effector cells, often accompanied by further BCR/Ig diversification *via* somatic hypermutation (SHM) and class switch recombination (CSR) (Chandra et al. 2015). SHM and CSR provide the molecular bases for generating high-affinity and isotype-switched BCRs/Igs, respectively (Methot and Di Noia 2017). At the cellular level, the combined effect of BCR engagement and helper T cell-derived signals induces the formation of specialized microstructures known as germinal centers (GCs), where activated B cells undergo a major proliferative burst, selection of high-affinity BCR variants, and differentiation into either antibody-secreting cells (ASCs, plasmablasts (PBs) and plasma cells (PCs)) or memory B cells (Victora and Nussenzweig 2022). B cell activation can also lead to PB generation at extrafollicular sites, which are also characterized by B cell proliferation and represent the main source of ASCs in T-cell independent responses (Elsner and Shlomchik 2020). The generation of PBs and long-lived PCs capable of secreting high-affinity Igs of different classes provides the foundation for the establishment of protective humoral responses.

43 RIF1 (Rap1-Interacting Factor 1 Homolog / Replication Timing Regulatory Factor 1)
44 is a multifunctional protein initially identified in budding yeast as a regulator of
45 telomere length homeostasis (Hardy et al. 1992). In mammalian cells, RIF1
46 contributes to preserving genome stability during both DNA replication and repair.
47 Under conditions of DNA replication stress, RIF1 protects nascent DNA at stalled
48 forks from degradation, facilitating their timely restart (Ray Chaudhuri et al. 2016;
49 Garzón et al. 2019; Mukherjee et al. 2019; Balasubramanian et al. 2022). During the
50 repair of DNA double-strand breaks (DSBs), RIF1 participates in the 53BP1-Shieldin
51 cascade that protects the broken DNA ends against nucleolytic resection, thus
52 influencing the choice of which DSB repair pathway to engage (Chapman et al.
53 2013; Di Virgilio et al. 2013; Escribano-Díaz et al. 2013; Feng et al. 2013;
54 Zimmermann et al. 2013). In addition to these genome-protective functions, RIF1
55 plays a central role in the control of DNA replication timing programs in both yeast
56 and higher eukaryotes (Yamazaki et al. 2012; Foti et al. 2016; Gnan et al. 2021;
57 Malzl et al. 2023). Several studies have also implicated RIF1 in early mouse
58 development (Dan et al. 2014; Liu et al. 2023; Zhang et al. 2022; Li et al. 2015,
59 2022). This role appears independent from RIF1's various activities in DNA
60 metabolism, and is mediated by its ability to modulate the transcriptional networks
61 responsible for embryonic stem cell state stability and differentiation (Dan et al.
62 2014; Liu et al. 2023; Zhang et al. 2022; Li et al. 2015, 2022).
63
64 Isotype diversification by CSR occurs *via* a deletional recombination reaction at the
65 Ig heavy chain (*Igh*) locus, which replaces the constant (C) region of the IgM/IgD
66 basal isotype with one of the downstream C regions encoding for the different
67 classes (IgG, IgE or IgA) (Methot and Di Noia 2017). The process necessitates the

formation of programmed *Igh* DSBs, which are physiologically protected from extensive resection to enable productive repair events and CSR (Saha et al. 2021). Due to its ability to inhibit DSB end processing, RIF1 is required for repair of *Igh* breaks, and hence for efficient Ig isotype diversification (Chapman et al. 2013; Di Virgilio et al. 2013; Escribano-Díaz et al. 2013). In this study, we report a novel role for RIF1 in the regulation of humoral immunity. We discovered that RIF1 expression is upregulated in mature B cells following activation, where it binds promoters of genes involved in B cell function and differentiation. RIF1 deficiency skews the transcriptional profile of activated B cells towards PBs and PCs, and is associated with an accelerated differentiation into ASCs both *ex* and *in vivo*. RIF1 directly binds several BLIMP1 target genes and counteracts their premature repression. Thus, by shaping mature B cell identity after activation, RIF1 contributes an additional regulatory layer to the B cell differentiation program that is essential to establish secreted antibody diversity.

Results and Discussion

Rif1 expression is regulated during B cell differentiation

To assess whether RIF1 contributes functions beyond the regulation of DNA end processing and repair in B cells, we first monitored *Rif1* expression levels across B cell lineage developmental stages using the Immunological Genome Project (ImmGen) transcriptomics data (The Immunological Genome Project et al. 2020). *Rif1* expression varied considerably in the different B cell subtypes, with GC cells exhibiting the highest levels (Fig. 1A). In contrast, the expression of RIF1's interactor partner in DNA repair, 53BP1, did not show any major changes during B cell development and differentiation (Fig. 1A). In addition, *ex vivo* activation of isolated naïve B cells (Fig. 1B and S1) resulted in upregulation of *Rif1*, but not *Tp53bp1*, transcript levels, regardless of the stimulation condition (LPS and IL-4 (LI); LPS, BAFF and TGFβ (LBT); or LPS (L)) and resulting isotype switching (IgG1, IgG2b, or IgG3, respectively) (Fig. 1, B and C). We concluded that, in contrast to *Tp53bp1*, *Rif1* expression is induced following activation of mature B cells both *in* and *ex vivo*.

RIF1 deficiency skews the transcriptional profile of activated B cells towards ASCs

We next assessed the consequences of RIF1 deficiency on the mature B cell transcriptome. To do so, we employed splenocyte cultures from $Rif1^{F/F}Cd19^{Cre/+}$ mice (Fig. 2A), which conditionally ablate *Rif1* expression at the immature B cell stage (Di Virgilio et al. 2013). Comparative assessment of the transcriptional profiles at different time points after activation identified only a limited number of considerably deregulated genes in the absence of RIF1 (N° genes with log2 FC < -1 and > 1 = 0,

107 105, and 47 at 48, 72, and 96 h, respectively) (Fig. 2B, S2, A and B, and Table S1).
108 Furthermore, the expression of the mature B cell identity transcriptional regulators
109 (*Pax5*, *Ebf1*, *Foxo1,* and *Bach2*) was not affected (Fig. S2C). These findings indicate
110 that RIF1 is largely dispensable for the induction of the stimulation-dependent
111 mature B cell program.
112
113 Activation of isolated splenocytes with specific stimuli recapitulates several features
114 of terminal B cell differentiation (Shi et al. 2015; Minnich et al. 2016). Therefore, we
115 next assessed the status of the key factors driving the ASC program (*Prdm1*, *Irf4*,
116 and *Xbp1*). We found a near 2-fold increase in *Prdm1* transcript levels at 96 h after
117 activation (Fig. 2B and S2C). Since the *Prdm1*-encoded transcription factor BLIMP1
118 is required for the differentiation of pre-PBs into PBs and PCs (Kallies et al. 2007;
119 Minnich et al. 2016), we cross-referenced the list of differentially expressed genes
120 (DEG, adjusted p-value < 0.05) from $Rif1^{F/F}Cd19^{Cre/+}$ activated B cells (Table S1)
121 with the PB and PC signatures (Minnich et al. 2016) (see Supplemental Materials
122 and Methods). We observed a significant overlap between DEGs and the
123 corresponding up-/down-regulated gene set in the ASC signatures, with the
124 tendency being more pronounced for the down-regulated datasets (Fig. 2C, S2D,
125 and Table S2). We concluded that RIF1 deficiency in activated B cells results in a
126 deregulated expression profile enriched in genes normally expressed in terminally
127 differentiated B cells.
128
129 **RIF1 limits the *ex vivo* differentiation of activated B cells into PBs and PC-like**
130 **cells**

131 Stimulation of naïve B cells with LPS and IL-4 induces their *ex vivo* differentiation into
132 PBs at later time points after activation (96 h, (Scharer et al. 2018)). Therefore, we
133 asked whether the skewed transcriptional profile exhibited by RIF1-deficient B cells
134 reflects an altered potential for terminal differentiation. To this end, we compared the
135 formation of PBs (CD138^{+}) in LI-stimulated B cells from *Cd19^{Cre}* and *Rif1$^{F/F}$Cd19^{Cre}*
136 mice at 96 h post-activation. We found an over two-fold increase in the percentage of
137 CD138^{+} cells in RIF1-deficient samples compared to controls (Fig. 3A), thus
138 indicating that the absence of RIF1 facilitates the *ex vivo* generation of PBs.
139
140 Currently, no *in vitro* setting can fully recapitulate the complexity of PC differentiation
141 and function. However, the induced GC B (iGB) culture system ideated by Nojima *et*
142 *al.* mimics the T cell-dependent generation of GC B cells and enables the *in vitro*
143 manipulation of their fates into either memory- or long-lived PC-like cells (Nojima et
144 al. 2011) (Fig. 3B). We took advantage of this system to assess the contribution of
145 RIF1 to the terminal differentiation of activated B cells *ex vivo*. At the GC-like
146 phenotype stage (four days stimulation with IL-4 on CD40L- and BAFF-expressing
147 feeder cells), RIF1 deficiency resulted in the expected severe defect in CSR (Fig. 3,
148 B and C) (Chapman et al. 2013; Di Virgilio et al. 2013; Escribano-Díaz et al. 2013).
149 However, and in agreement with their increased potential to differentiate into PBs
150 (Fig. 3A), *Rif1$^{F/F}$Cd19^{Cre}* B cells showed a near two-fold increase in the percentage
151 of PC-like cells after prolonged culturing in the presence of IL-21 (Fig. 3, B and D).
152 Altogether, these data indicate that RIF1 deficiency promotes the *ex vivo*
153 differentiation of activated B cells to PBs and PC-like cells.
154
155 **RIF1 curtails plasma cell formation following immunization**

156 We next investigated whether RIF1 influences the differentiation of activated B cells
157 into PCs also *in vivo*. To this end, we analyzed the PC compartment of control and
158 *Rif1*$^{F/F}$*Cd19*$^{Cre/+}$ mice immunized with the T-cell-dependent antigen 4-Hydroxy-3-
159 nitrophenylacetyl hapten conjugated to Chicken Gamma Globulin (NP-CGG) (Fig.
160 4A). *Rif1*$^{F/F}$*Cd19*^{Cre} mice showed a consistent increase in the proportion of PCs
161 (TACI^{+}CD138^{+}AA4.1^{+}MHCII^{-}) within the ASC population compared to controls in
162 both spleen and bone marrow at earlier time points post-immunization (day 7 and 14
163 in the spleen and day 14 in the bone marrow) (Fig. 4B and S3). The phenotype was
164 no longer observed in either compartment at later time points (day 28, Fig. 4B) nor in
165 unimmunized mice (Fig. S4). These finding indicate that RIF1 deletion removes a
166 physiological restraint imposed over the terminal differentiation of mature B cells,
167 which, though concealed under steady-state conditions *in vivo*, the phenotype is
168 readily detectable at the systemic level upon immunization.
169
170 Several recent studies have proposed that, besides SHM, B cell receptor (BCR)
171 diversification *via* CSR can also influence the differentiation outcome of GC B cells
172 (Gómez-Escolar et al. 2022; Kometani et al. 2013; Gitlin et al. 2016; King et al.
173 2021). Given the strict dependency of CSR on RIF1 (Chapman et al. 2013; Di Virgilio
174 et al. 2013; Escribano-Díaz et al. 2013), it is tempting to speculate that the skewed
175 differentiation potential of RIF1-deficient B cells might represent an indirect
176 consequence of altered BCR signaling or GC recruitment caused by defective
177 isotype switching. However, the *ex vivo* recapitulation of the differentiation
178 phenotype (Fig. 3A), in the absence of BCR engagement and physiological
179 microenvironmental cues, argues against this possibility and in favor of a cell-
180 intrinsic role of RIF1 in shaping B cell identity during late differentiation.

181 **RIF1 counteracts the premature repression of BLIMP1 target genes**

182 To uncover the mechanism underlying RIF1 ability to restrain terminal B cell
183 differentiation, we first monitored the genome-wide occupancy of RIF1 in activated B
184 cells from *Rif1*$^{FH/FH}$ mice under the same stimulation conditions employed for the *ex*
185 *vivo* transcriptional analyses (Fig. 5A, (Malzl et al. 2023)). *Rif1*$^{FH/FH}$ splenocytes
186 express physiological levels of a knock-in 1×Flag-2×Hemagglutinin-tagged version of
187 RIF1 (RIF1^{FH},(Cornacchia et al. 2012)) that supports its roles in mouse embryonic
188 fibroblasts, embryonic stem cells, and B cells (Cornacchia et al. 2012; Foti et al.
189 2016; Di Virgilio et al. 2013). Interestingly, the vast majority of RIF1 peaks
190 colocalized with promoters (56,4 %) and distal intergenic regions (25,4 %) (Fig. 5B).
191 We next assessed the functional significance of both proximal- and distal-to-gene
192 RIF1-binding events. We identified several categories of genes associated with the
193 regulation of lymphocyte activation, function, and differentiation (Fig. S5A and Table
194 S3). Altogether, these findings indicate that in activated B cells, RIF1 associates with
195 cis-regulatory elements of genes involved in the modulation of the adaptive immune
196 response.

197

198 We next explored the relationship of RIF1 with BLIMP1, the key transcriptional
199 regulator of terminal B cell differentiation (Minnich et al. 2016; Malzl et al. 2023). To
200 this end, we first assessed their relative genome occupancy by comparing RIF1
201 peaks (Fig. 5B) with BLIMP1-bound regions in activated B cells (see Supplemental
202 Materials and Methods). We found that 1300 genomic regions (corresponding to
203 1144 genes) were co-occupied by the two factors (Fig. 5C), and they primarily
204 comprised active genes (Fig. S5B), many of which are involved in lymphocyte
205 activation and differentiation (Fig. S5C and Table S3). Since genome occupancy is

206 not indicative *per se* of a gene regulatory activity, we next asked whether RIF1
207 deficiency affects the transcriptional status of BLIMP1 targets, which are defined as
208 BLIMP1-occupied genes that are either up- (repressed, 121 targets) or down-
209 (activated, 93 targets) regulated following its ablation (Minnich et al. 2016). We found
210 that several BLIMP1-activated genes were significantly up-regulated in
211 *Rif1*$^{F/F}$*Cd19*$^{Cre/+}$ cells at 96 h post-activation (Fig. 5D), which is in agreement with the
212 increased percentage of PBs in these cultures (Fig. 3A). More interestingly, BLIMP1-
213 repressed targets were tendentially downregulated in the absence of RIF1 (Fig. 5D).
214 The phenotype was evident not only at 96 h, but also at 72 h post-activation (Fig.
215 5D), before the physiological appearance of phenotypically-defined PBs (Scharer et
216 al. 2018). Furthermore, a considerable portion of these genes is occupied by RIF1 in
217 wild-type (*Rif1*$^{FH/FH}$) cells (Fig. S5D), which suggests a direct modulatory function.
218 Altogether, these findings indicate that RIF1 supports the expression of several
219 genes that are physiologically down-regulated by BLIMP1 as part of the
220 transcriptional program promoting B cell differentiation into ASCs.
221
222 Collectively, our results support a model where RIF1 serves as a gatekeeper of B
223 cell identity during terminal differentiation through its capacity to counteract the
224 premature repression of BLIMP1 target genes following activation. This gatekeeping
225 role has important implications for the pathological consequences of deregulated
226 plasma cell generation. Whilst producing a diverse Ig-switched repertoire enables
227 effective antibody-mediated responses, tight regulation and fine tuning of late B cell
228 differentiation is essential to counteract the development of autoimmunity and PC-
229 derived malignancies (Elkon and Casali 2008; Barwick et al. 2019; García-Sanz et
230 al. 2016). Hence, by enabling *Igh* diversification *via* CSR while exerting a modulatory

231 function on PC differentiation, RIF1 integrates key requirements for the

232 establishment of protective humoral immunity.

233 **Materials & Methods**

234

235 **Mice and derived primary cell cultures**

236 *Rif1*$^{FH/FH}$ (Cornacchia et al. 2012), *Cd19*^{Cre} (Rickert et al. 1997) and *Rif1*$^{F/F}$*Cd19*$^{Cre/+}$
237 (Di Virgilio et al. 2013) mice were previously described and maintained on a C57BL/6
238 background. Mice were kept in a specific pathogen-free (SPF) barrier facility and all
239 experiments were performed in compliance with the European Union (EU) directive
240 2010/63/EU, and in agreement with Landesamt für Gesundheit und Soziales
241 directives (LAGeSo, Berlin, Germany). Mice of both genders were used for the
242 experiments.
243 Resting B lymphocytes were isolated from mouse spleens using anti-CD43
244 MicroBeads (Miltenyi Biotec), and grown in RPMI 1640 medium (Life Technologies)
245 supplemented with 10% fetal bovine serum (FBS, Sigma-Aldrich), 10 mM HEPES
246 (Life Technologies), 1 mM Sodium Pyruvate (Life Technologies), 1X Antibiotic
247 Antimycotic (Life Technologies), 2 mM L-Glutamine (Life Technologies), and 1X 2-
248 Mercaptoethanol (Life Technologies) at 37 °C and 5% CO2 levels. Naïve B cells
249 were activated by addition of 5-25 μg/ml LPS (Sigma-Aldrich) and 5 ng/ml of mouse
250 recombinant IL-4 (Sigma-Aldrich) (L-I), or 5 μg/ml LPS, 10 ng/ml BAFF (PeproTech)
251 and 2 ng/ml TGFβ (L-B-T), or 5 μg/ml LPS only (L).

252

253 **RNA-Seq**

254 For each RNA-Seq dataset, the analysis was performed on three mice per genotype.
255 Splenocytes were cultured in LPS and IL-4 (LI), LPS, BAFF and TGFβ (LBT), or LPS
256 (L), and cells were collected at the indicated time points by centrifugation. RNA was
257 extracted with TRIzol (Invitrogen) according to manufacturer's instructions, and

258 ribosomal RNA was depleted using Ribo-Zero Gold rRNA Removal Kit (Illumina) for
259 all datasets except for the RNA-Seq analysis in naïve versus L-I/L-B-T/L-activated
260 splenocytes from WT mice (Fig. 1 and S1), for which RNase H (Epicentre) treatment
261 was used. Libraries were prepared with TruSeq Stranded Total RNA Library Prep Kit
262 Gold (Illumina), and run in one lane on a flow cell of NovaSeq 6000 SP (Illumina).
263

264 **ChIP-Seq**

265 ChIP-Seq for RIF1 in LPS and IL-4-stimulated splenocyte cultures was previously
266 described (Malzl et al. 2023). H3K4me3 ChIP-Seq was performed in splenocytes
267 activated with LPS and IL-4 for 72 h, and employed anti-H3K4me3 antibody (abcam,
268 ab8580) for the ChIP part of the previously described protocol (Pavri et al. 2010). For
269 H3K27me3 ChIP-Seq, we used H3K27me3 antibody (Cell Signalling, C36B11), and
270 2.5% human shared chromatin was spiked into all samples as an internal reference
271 for normalization (Bonhoure et al. 2014).
272

273 **B cell development and differentiation analyses**

274 For analysis of CSR in *ex vivo* cultures, cell suspensions were stained with anti-
275 IgG1-APC (BD Biosciences), anti-IgG3-Biotin and Streptavidin-APC (BD
276 Biosciences), or anti-IgG2b-PE (BioLegend). For analysis of plasmablast
277 differentiation *ex vivo*, isolated naïve splenic B cells were cultured at a density of 0,5
278 x 10^6 cells/ml in the presence of 25 μg/ml LPS and 5 ng/ml IL-4 and stained with
279 anti-CD138 (BioLegend). For analysis of plasma cell-like differentiation *ex vivo*, the
280 induced GC B (iGB) culture system was used as described before (Nojima et al.
281 2011; Haniuda and Kitamura 2019). Briefly, 40LB feeder cells (Balb/c 3T3 cell line
282 expressing exogenous CD40-ligand (CD40L) and B-cell activating factor (BAFF))

283 were irradiated with 80 Gy and co-cultured with primary splenic B cells for 4 days in
284 high glucose DMEM medium (Gibco) supplemented with 10% FBS, 10 mM HEPES,
285 1 mM Sodium Pyruvate, 1X Pen/Strep (Life Technologies), 1x MEM Non-Essential
286 Amino Acids (Life Technologies), 2 mM L-Glutamine, 1X 2-Mercaptoethanol and 1
287 ng/ml IL-4 at 37 °C and 5% CO_2 levels. On day 4, cells were harvested, washed one
288 time with PBS and re-plated in a newly irradiated 40LB feeder layer in the presence
289 of 10 ng/ml IL-21 (PeproTech) for the next 4 days. For assessing CSR and plasma
290 cell-like differentiation on day 4 and 8, 1 x 10^6 B cells were washed one time with
291 FACS buffer (PBS supplemented with 1% FCS and 1 mM EDTA), blocked with
292 TruStain fcX (BioLegend) for 10 min at 4° C and stained with the respective
293 antibodies as stated above. 1 µg/ml of propidium iodide (PI) was used for live/dead
294 cell staining.
295 For analysis of the plasma cell compartment *in vivo*, 8-14 week-old mice were
296 sacrificed to isolate the spleen and tibia. Single cell suspensions were incubated for
297 2 min with ACK buffer (Gibco) for red blood cell lysis. For surface staining, 5-7 × 10^6
298 cells were first blocked with TruStain fcX for 10 min at 4 °C and then stained for
299 CD138, CD267/ TACI (BD Pharmingen), MHC-II (Biolegend) and CD93/AA4.1
300 (Biolegend) 20 min at 4° C. Cells were resuspended in FACS buffer containing PI
301 and analyzed. Immunization was performed by intraperitoneal injection of 100 µg of
302 NP-CGG (Biosearch Technologies; ratio 10-20) precipitated in alum (Sigma).
303 All samples were acquired on a LSRFortessa cell analyzer (BD Biosciences).
304
305 **Data availability**
306 All RNA-Seq datasets reported in this study, and H3K4me3 and H3K27me3 ChIP-
307 Seq data have been deposited in the GEO repository under accession number

308 GSE237560 (token for editor and reviewers: anqtcskkfbqxjel).The transcriptional
309 signatures of activated B cells, PBs, and PCs have been defined using the
310 corresponding (and naïve B cells for baseline comparison) RNA-Seq datasets from
311 ((Minnich et al. 2016), GSE71698). RIF1 ChIP-Seq was previously reported ((Malzl
312 et al. 2023), GSE228880). The BLIMP1-bound regions in activated B cells were
313 defined based on the BLIMP1 Bio-ID dataset from ((Minnich et al. 2016),
314 GSE71698). The lists of BLIMP1-activated and -repressed targets have been
315 previously described (Minnich et al. 2016). Details of data analyses are described in
316 the Supplemental Materials and Methods file.

Competing Interest Statement

The authors declare no competing interests.

Acknowledgments

We thank all members of the Di Virgilio lab for discussion; L. Keller and T. Rüster (Di Virgilio lab, MDC, Berlin) for genotyping; W. Winkler (Janz/Mathas and K. Rajewsky labs, MDC) for *in vivo* protocols; and D. Pasini (IEO, Milan) and G. Gargiulo (MDC) for their valuable feedback. Figure schematics were created using images from Biorender. The project was funded by the Helmholtz-Gemeinschaft Zukunftsthema "Immunology and Inflammation" ZT-0027 (to M.D.V.) and the Initiative and Networking Fund of the Helmholtz Association (to M.D.V.).

Author contributions: A.R. and E.K. conceived the project idea, designed and performed experiments; M.B.L. and V.D.B prepared the RNA-seq libraries; A.R. analyzed all high-throughput sequencing data; R.A. contributed to the sequencing data analysis; R.P. engaged in active discussions on the study; M.D.V. secured the funding for the project, supervised all aspects of the study, and wrote the manuscript; A.R. and E.K. reviewed and edited the manuscript.

References

Balasubramanian S, Andreani M, Andrade JG, Saha T, Sundaravinayagam D, Garzón J, Zhang W, Popp O, Hiraga S, Rahjouei A, et al. 2022. Protection of nascent DNA at stalled replication forks is mediated by phosphorylation of RIF1 intrinsically disordered region eds. A. Aguilera and J.K. Tyler. *eLife* **11**: e75047.

Barwick BG, Gupta VA, Vertino PM, Boise LH. 2019. Cell of Origin and Genetic Alterations in the Pathogenesis of Multiple Myeloma. *Front Immunol* **10**: 1121.

Bonhoure N, Bounova G, Bernasconi D, Praz V, Lammers F, Canella D, Willis IM, Herr W, Hernandez N, Delorenzi M, et al. 2014. Quantifying ChIP-seq data: a spiking method providing an internal reference for sample-to-sample normalization. *Genome Res* **24**: 1157–1168.

Chandra V, Bortnick A, Murre C. 2015. AID Targeting: Old Mysteries and New Challenges. *Trends Immunol* **36**: 527–535.

Chapman JR, Barral P, Vannier J-B, Borel V, Steger M, Tomas-Loba A, Sartori AA, Adams IR, Batista FD, Boulton SJ. 2013. RIF1 Is Essential for 53BP1-Dependent Nonhomologous End Joining and Suppression of DNA Double-Strand Break Resection. *Molecular Cell* **49**: 858.

Cornacchia D, Dileep V, Quivy J-P, Foti R, Tili F, Santarella-Mellwig R, Antony C, Almouzni G, Gilbert DM, Buonomo SBC. 2012. Mouse Rif1 is a key regulator of the replication-timing programme in mammalian cells. *The EMBO Journal* **31**: 3678–3690.

Dan J, Liu Y, Liu N, Chiourea M, Okuka M, Wu T, Ye X, Mou C, Wang L, Wang L, et al. 2014. Rif1 maintains telomere length homeostasis of ESCs by mediating heterochromatin silencing. *Dev Cell* **29**: 7–19.

Di Virgilio M, Callen E, Yamane A, Zhang W, Jankovic M, Gitlin AD, Feldhahn N, Resch W, Oliveira TY, Chait BT, et al. 2013. Rif1 Prevents Resection of DNA Breaks and Promotes Immunoglobulin Class Switching. *Science* **339**: 10.1126/science.1230624.

Elkon K, Casali P. 2008. Nature and functions of autoantibodies. *Nat Clin Pract Rheumatol* **4**: 491–498.

Elsner RA, Shlomchik MJ. 2020. Germinal Center and Extrafollicular B Cell Responses in Vaccination, Immunity, and Autoimmunity. *Immunity* **53**: 1136–1150.

Escribano-Díaz C, Orthwein A, Fradet-Turcotte A, Xing M, Young JTF, Tkáč J, Cook MA, Rosebrock AP, Munro M, Canny MD, et al. 2013. A Cell Cycle-Dependent Regulatory Circuit Composed of 53BP1-RIF1 and BRCA1-CtIP Controls DNA Repair Pathway Choice. *Molecular Cell* **49**: 872–883.

Feng L, Fong K-W, Wang J, Wang W, Chen J. 2013. RIF1 Counteracts BRCA1-mediated End Resection during DNA Repair *. *Journal of Biological Chemistry* **288**: 11135–11143.

Foti R, Gnan S, Cornacchia D, Dileep V, Bulut-Karslioglu A, Diehl S, Buness A, Klein FA, Huber W, Johnstone E, et al. 2016. Nuclear Architecture Organized by Rif1 Underpins the Replication-Timing Program. *Mol Cell* **61**: 260–273.

García-Sanz R, Jiménez C, Puig N, Paiva B, Gutiérrez NC, Rodríguez-Otero P, Almeida J, San Miguel J, Orfão A, González M, et al. 2016. Origin of Waldenstrom's macroglobulinaemia. *Best Pract Res Clin Haematol* **29**: 136–147.

Garzón J, Ursich S, Lopes M, Hiraga S, Donaldson AD. 2019. Human RIF1-Protein Phosphatase 1 Prevents Degradation and Breakage of Nascent DNA on Replication Stalling. *Cell Reports* **27**: 2558-2566.e4.

Gitlin AD, von Boehmer L, Gazumyan A, Shulman Z, Oliveira TY, Nussenzweig MC. 2016. Independent Roles of Switching and Hypermutation in the Development and Persistence of B Lymphocyte Memory. *Immunity* **44**: 769–781.

Gnan S, Flyamer IM, Klein KN, Castelli E, Rapp A, Maiser A, Chen N, Weber P, Enervald E, Cardoso MC, et al. 2021. Nuclear organisation and replication timing are coupled through RIF1–PP1 interaction. *Nat Commun* **12**: 2910.

Gómez-Escolar C, Serrano-Navarro A, Benguria A, Dopazo A, Sánchez-Cabo F, Ramiro AR. 2022. Single cell clonal analysis identifies an AID-dependent pathway of plasma cell differentiation. *EMBO Rep* **23**: e55000.

Haniuda K, Kitamura D. 2019. Induced Germinal Center B Cell Culture System. *Bio Protoc* **9**: e3163.

Hardy CF, Sussel L, Shore D. 1992. A RAP1-interacting protein involved in transcriptional silencing and telomere length regulation. *Genes Dev* **6**: 801–814.

Kallies A, Hasbold J, Fairfax K, Pridans C, Emslie D, McKenzie BS, Lew AM, Corcoran LM, Hodgkin PD, Tarlinton DM, et al. 2007. Initiation of Plasma-Cell Differentiation Is Independent of the Transcription Factor Blimp-1. *Immunity* **26**: 555–566.

King HW, Orban N, Riches JC, Clear AJ, Warnes G, Teichmann SA, James LK. 2021. Single-cell analysis of human B cell maturation predicts how antibody class switching shapes selection dynamics. *Sci Immunol* **6**: eabe6291.

Kometani K, Nakagawa R, Shinnakasu R, Kaji T, Rybouchkin A, Moriyama S, Furukawa K, Koseki H, Takemori T, Kurosaki T. 2013. Repression of the transcription factor Bach2 contributes to predisposition of IgG1 memory B cells toward plasma cell differentiation. *Immunity* **39**: 136–147.

Li L, Li P, Chen J, Li L, Shen Y, Zhu Y, Liu J, Lv L, Mao S, Chen F, et al. 2022. Rif1 interacts with non-canonical polycomb repressive complex PRC1.6 to regulate mouse embryonic stem cells fate potential. *Cell Regen* **11**: 25.

Li P, Ma X, Adams IR, Yuan P. 2015. A tight control of Rif1 by Oct4 and Smad3 is critical for mouse embryonic stem cell stability. *Cell Death Dis* **6**: e1588.

Lin SG, Ba Z, Alt FW, Zhang Y. 2018. Chapter Three - RAG Chromatin Scanning During V(D)J Recombination and Chromatin Loop Extrusion are Related Processes. In *Advances in Immunology* (ed. F. Alt), Vol. 139 of, pp. 93–135, Academic Press https://www.sciencedirect.com/science/article/pii/S0065277618300282 (Accessed May 17, 2023).

Liu C, Yu P, Ren Z, Yao F, Wang L, Hu G, Li P, Zhao Q. 2023. Rif1 Regulates Self-Renewal and Impedes Mesendodermal Differentiation of Mouse Embryonic Stem Cells. *Stem Cell Rev Rep*.

Malzl D, Peycheva M, Rahjouei A, Gnan S, Klein KN, Nazarova M, Schoeberl UE, Gilbert DM, Buonomo SCB, Virgilio MD, et al. 2023. *RIF1 regulates replication origin activity and early replication timing in B cells*. Genetics http://biorxiv.org/lookup/doi/10.1101/2023.03.31.535086 (Accessed April 16, 2023).

Methot SP, Di Noia JM. 2017. Molecular Mechanisms of Somatic Hypermutation and Class Switch Recombination. *Adv Immunol* **133**: 37–87.

Minnich M, Tagoh H, Bönelt P, Axelsson E, Fischer M, Cebolla B, Tarakhovsky A, Nutt SL, Jaritz M, Busslinger M. 2016. Multifunctional role of the transcription factor Blimp-1 in coordinating plasma cell differentiation. *Nat Immunol* **17**: 331–343.

Mukherjee C, Tripathi V, Manolika EM, Heijink AM, Ricci G, Merzouk S, de Boer HR, Demmers J, van Vugt MATM, Ray Chaudhuri A. 2019. RIF1 promotes replication fork protection and efficient restart to maintain genome stability. *Nat Commun* **10**: 3287.

Nemazee D. 2017. Mechanisms of central tolerance for B cells. *Nat Rev Immunol* **17**: 281–294.

Nojima T, Haniuda K, Moutai T, Matsudaira M, Mizokawa S, Shiratori I, Azuma T, Kitamura D. 2011. In-vitro derived germinal centre B cells differentially generate memory B or plasma cells in vivo. *Nature Communications 2011 2:1* **2**: 1–11.

Pavri R, Gazumyan A, Jankovic M, Di Virgilio M, Klein I, Ansarah-Sobrinho C, Resch W, Yamane A, San-Martin BR, Barreto V, et al. 2010. Activation-Induced Cytidine Deaminase Targets DNA at Sites of RNA Polymerase II Stalling by Interaction with Spt5. *Cell* **143**: 122–133.

Ray Chaudhuri A, Callen E, Ding X, Gogola E, Duarte AA, Lee J-E, Wong N, Lafarga V, Calvo JA, Panzarino NJ, et al. 2016. Replication fork stability confers chemoresistance in BRCA-deficient cells. *Nature* **535**: 382–387.

Rickert RC, Roes J, Rajewsky K. 1997. B lymphocyte-specific, Cre-mediated mutagenesis in mice. *Nucleic Acids Res* **25**: 1317–1318.

Saha T, Sundaravinayagam D, Di Virgilio M. 2021. Charting a DNA Repair Roadmap for Immunoglobulin Class Switch Recombination. *Trends Biochem Sci* **46**: 184–199.

Scharer CD, Barwick BG, Guo M, Bally APR, Boss JM. 2018. Plasma cell differentiation is controlled by multiple cell division-coupled epigenetic programs. *Nat Commun* **9**: 1698.

Shi W, Liao Y, Willis SN, Taubenheim N, Inouye M, Tarlinton DM, Smyth GK, Hodgkin PD, Nutt SL, Corcoran LM. 2015. Transcriptional profiling of mouse B cell terminal differentiation defines a signature for antibody-secreting plasma cells. *Nat Immunol* **16**: 663–673.

The Immunological Genome Project, Aguilar SV, Aguilar O, Allan R, Amir EAD, Angeli V, Artyomov MN, Asinovski N, Astarita J, Austen KF, et al. 2020. ImmGen at 15. *Nat Immunol* **21**: 700–703.

Victora GD, Nussenzweig MC. 2022. Germinal Centers. *Annual Review of Immunology* **40**: 413–442.

Yamazaki S, Ishii A, Kanoh Y, Oda M, Nishito Y, Masai H. 2012. Rif1 regulates the replication timing domains on the human genome. *EMBO J* **31**: 3667–3677.

Zhang W, Yao C, Luo Y, Li Q, Zhao Q, Zhao Y, Wang Y, Geng M, Wang Q, Xu M, et al. 2022. Rif1 and Hmgn3 regulate the conversion of murine trophoblast stem cells. *Cell Rep* **38**: 110570.

Zimmermann M, Lottersberger F, Buonomo SB, Sfeir A, De Lange T. 2013. 53BP1 Regulates DSB Repair Using Rif1 to Control 5′ End Resection. *Science* **339**: 700–704.

Supplemental Material

Supplemental_Fig_S1.pdf

Stimulation-dependent clustering of B cell transcriptomics profiles after *ex vivo* activation. Related to Figure 1.

Supplemental_Fig_S2.pdf

RIF1-deficiency alters the transcriptional landscape of activated B cells. Related to Figure 2.

Supplemental_Fig_S3.pdf

***Rif1*$^{F/F}$*Cd19*$^{Cre/+}$ mice exhibit physiological numbers of ASCs after immunization.** Related to Figure 4.

Supplemental_Fig_S4.pdf

RIF1 ablation does not result in detectable changes of the plasma cell compartment in steady state condition. Related to Figure 4.

Supplemental_Fig_S5.pdf

RIF1 and BLIMP1 co-occupied genomic regions comprise active genes involved in lymphocyte activation and differentiation. Related to Figure 5.

Supplemental_Table_S1.xlsx

Pairwise comparison of differentially regulated genes in control (*Cd19*$^{Cre/+}$) *versus Rif1*$^{F/F}$*Cd19*$^{Cre/+}$ splenocytes. Related to Figures 2 and S2.

Supplemental_Table_S2.xlsx

Lists of genes in the PB and PC transcriptional signatures that are differentially regulated in *Rif1*$^{F/F}$*Cd19*$^{Cre/+}$ activated B cells. Related to Figures 2 and S2.

Supplemental_Table_S3.xlsx

Lists of RIF1- and RIF1&BLIMP1-bound genes in the top GREAT gene ontology enrichment categories. Related to Figure S5.

Supplemental_Table_S4.xlsx

Lists of RIF1&BLIMP1 target genes. Related to Figure S5.

Supplemental_Materials_&_Methods.pdf

Data analysis and Softwares.

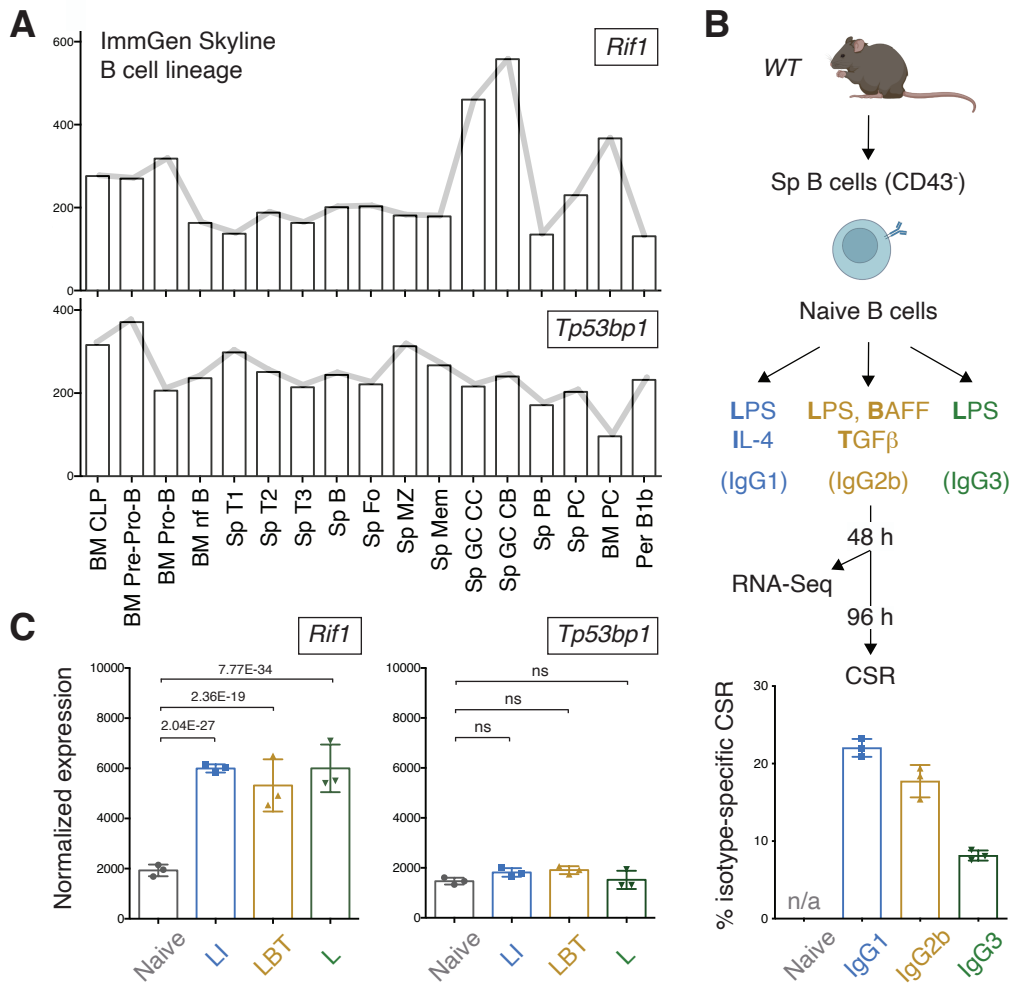

Figure 1. *Rif1* expression is dynamically regulated during late B cell differentiation. (A) Expression of *Rif1* (top) and *Tp53bp1* (bottom) genes across B cell lineage developmental stages as determined by the Immunological Genome Project (ImmGen) Skyline RNA-Seq analysis. BM: bone marrow; CLP: common lymphoid progenitor; nf: newly-formed; Sp: splenic; Fo: follicular; MZ: marginal zone; Mem: memory; GC: germinal center; CC: centrocytes; CB: centroblasts; PB: plasmablasts; PC: plasma cells; Per B1b: peritoneal B1b. (B) Top: Schematic representation of gene expression analysis in naïve B cells isolated from mouse spleens and stimulated *ex vivo* with LPS and IL-4 (LI cocktail), LPS, BAFF and TGFβ (LBT), or LPS only (L). Bottom: CSR efficiency to the corresponding isotype for each of the primary B cell cultures employed in the RNA-Seq analysis (n = 3 mice per stimulation condition). n/a: not applicable. (C) Expression of *Rif1* (left) and *Tp53bp1* (right) genes in naïve and LI/LBT/L-stimulated B cells. Expression values were normalized by DESeq2 and the adjusted p-value of significant differences between samples is indicated. ns: not significant.

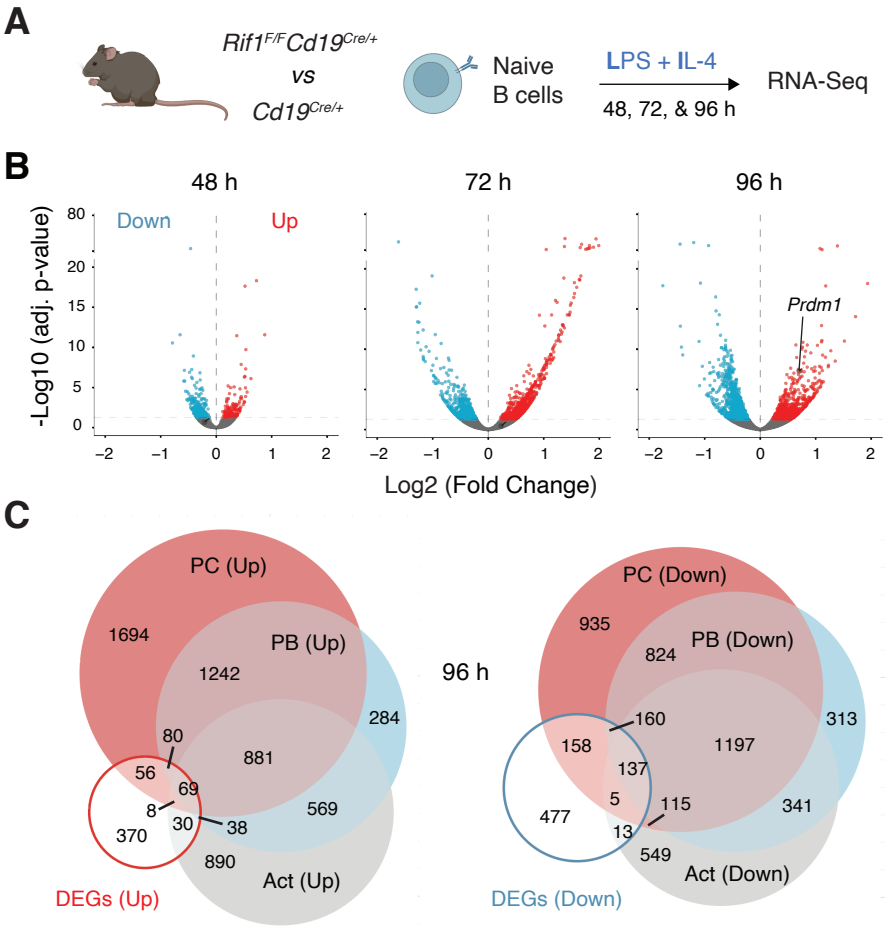

Figure 2. RIF1 deficiency skews the transcriptional profile of activated B cells towards ASCs. (A) Schematic representation of gene expression analysis in naïve B cells isolated from *Cd19*$^{Cre/+}$ and *Rif1*$^{F/F}$*Cd19*$^{Cre/+}$ mouse spleens and stimulated *ex vivo* with LI for 48, 72, and 96 h. For the 48 h time point, the analysis was performed also on LBT-stimulated cultures. (B) Volcano plots displaying differentially expressed genes between control and RIF1-deficient splenocytes. The blue and red dots represent transcripts down- and up-regulated (adjusted p-value <= 0.05, blue horizontal dotted line), respectively, in *Rif1*$^{F/F}$*Cd19*$^{Cre/+}$ cells. (C) Venn diagrams depicting the overlaps between genes up- (left) and down- (right) regulated in RIF1-deficient splenocytes at 96 h post-activation and the corresponding up-and down-regulated (over naïve B cells) categories in the activated (Act) B cell, PB, and PC transcriptional signatures (Minnich et al. 2016).

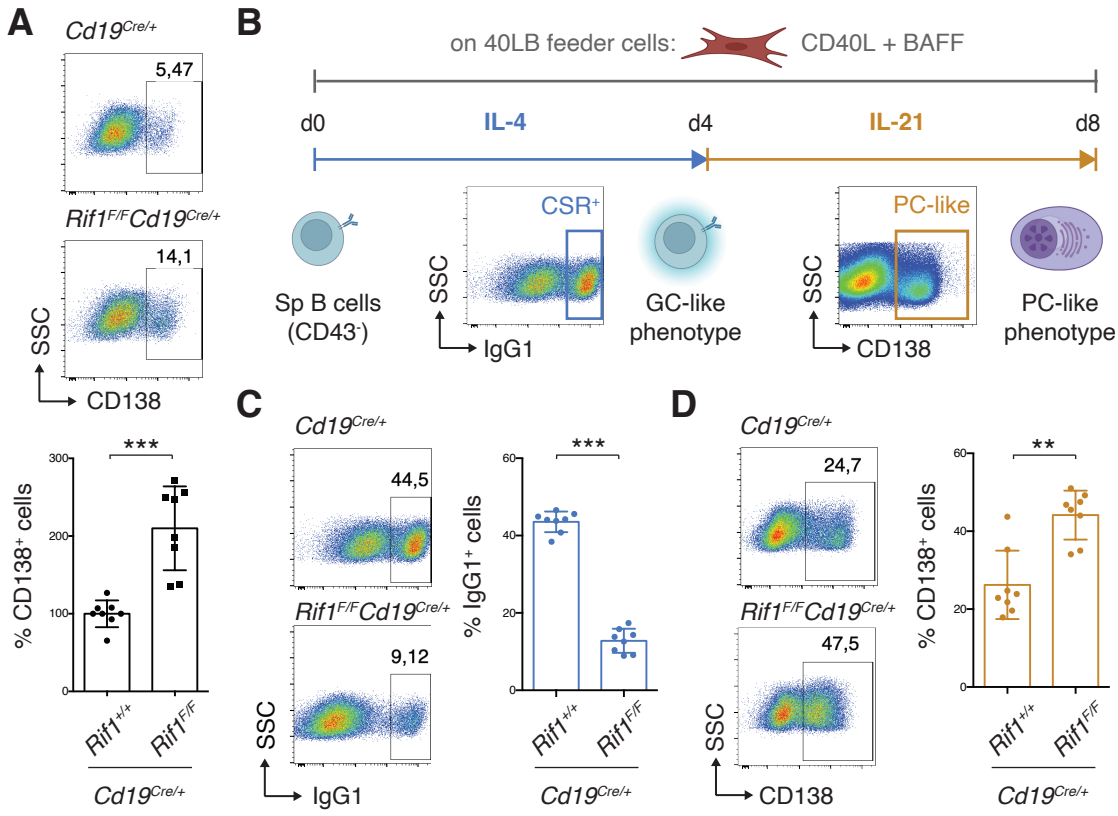

Figure 3. *Ex vivo* differentiation of activated B cells to PBs and PC-like cells is increased in the absence of RIF1. (A) Top: Representative flow cytometry plots measuring percentage of plasmablasts (CD138+) in splenocyte cultures of the indicated genotypes 96 h after activation with LI. Bottom: Summary graph for five independent experiments (n = eight mice per genotype), with % of CD138+ cells within each experiment normalized to the average of control mice (*Cd19*$^{Cre/+}$), which was set to 100%. (B) Schematic representation of the iGB (induced germinal center (GC) phenotype B) cell culture system for the *ex vivo* differentiation of splenic naïve B cells to GC- and plasma cell-like cells. CD40L: CD40 ligand; d: day; Sp: splenic; CSR+: class switched cells; PC: plasma cell. (C-D) Left: Representative flow cytometry plots measuring CSR to IgG1 (C) and percentage of plasmablasts (CD138+) (D) in splenocytes cultures of the indicated genotypes at day 4 (C) and 8 (D), respectively, of the iGB cell culture system shown in panel B. Right: Summary graphs for five independent experiments (n = eight mice per genotype). Significance in panels A, C and D was calculated with the Mann–Whitney U test, and error bars represent SD. ** = $p \leq 0.01$; *** = $p \leq 0.001$.

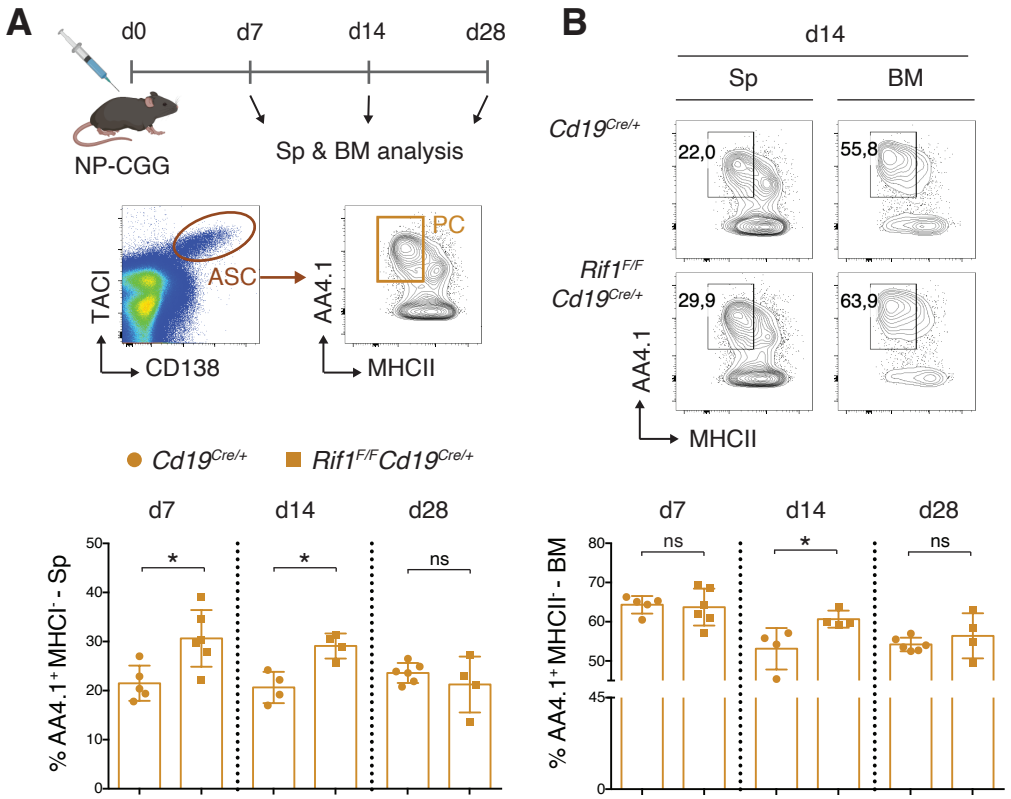

Figure 4. Ablation of RIF1 enhances plasma cell formation after immunization. (A) Schematic representation of the NP-CGG immunization protocol and gating strategy employed for the phenotypic analysis of the plasma cell compartment. d: day; NP-CGG: 4-hydroxy-3-nitrophenylacetyl hapten conjugated to Chicken Gamma Globulin; Sp: spleen; BM: bone marrow; ASC: antibody secreting cell; PC: plasma cell. (B) Top: Representative flow cytometry plots measuring percentage of plasma cells in spleens and bone marrows of mice of the indicated genotypes at day 14 after immunization. Bottom: Graphs summarizing the percentage of plasma cells in spleens (left) and bone marrows (right) for >= four mice per genotype and time point. Significance in panel B was calculated with the Mann–Whitney U test, and error bars represent SD. ns: not significant; * = $p \leq 0.05$.

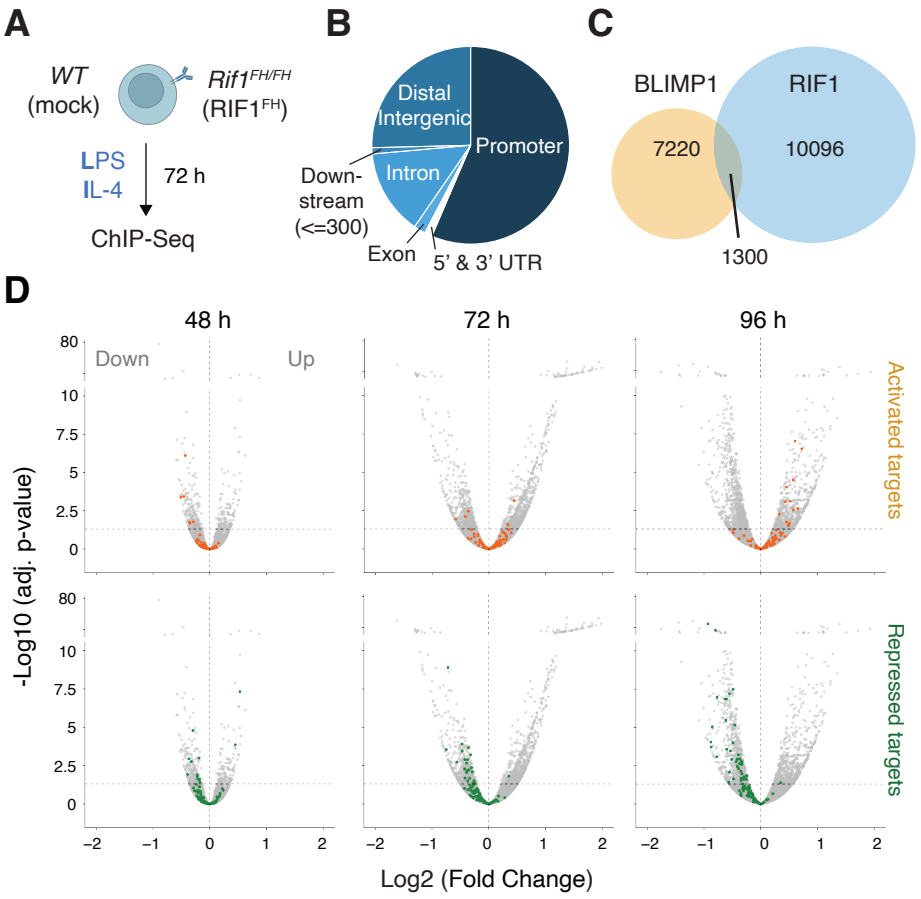

Figure 5. RIF1 counteracts the premature repression of BLIMP1 target genes. (A) Schematic representation of the ChIP-Seq analysis in mature B cells isolated from spleens of *Rif1*$^{FH/FH}$ mice and stimulated *ex vivo* with LI. (B) Genomic distribution of RIF1-occupied annotated regions. (C) Venn diagram depicting the overlap between RIF1- and BLIMP1-bound genomic regions in activated B cells. (D) Volcano plots displaying BLIMP1-activated (in orange, top) and -repressed (in green, bottom) target genes among the transcripts (in grey both up- and down-regulated) identified in the *Cd19*$^{Cre/+}$ *versus* *Rif1*$^{F/F}$*Cd19*$^{Cre/+}$ transcriptome analysis shown in Fig. 2. The horizontal dotted line in the plots denotes the adjusted p-value of 0.05.